

AD-A053 648

WEAPONS RESEARCH ESTABLISHMENT SALISBURY (AUSTRALIA)

F/6 19/4

INFLUENCE OF GRAVITY AND APPLIED SIDE FORCES ON THE STABILITY 0--ETC(U)

NOV 77 K H LLOYD, D P BROWN

WRE-TR-1906(W)

NL

UNCLASSIFIED

1 OF 1  
AD  
A053648



END  
DATE  
FILMED  
6 -78  
DDC



12 P.S.

AD A 053648

# DEPARTMENT OF DEFENCE

DEFENCE SCIENCE AND TECHNOLOGY ORGANISATION

WEAPONS RESEARCH ESTABLISHMENT

SALISBURY, SOUTH AUSTRALIA

TECHNICAL REPORT 1906 (W)

INFLUENCE OF GRAVITY AND APPLIED SIDE FORCES ON THE  
STABILITY OF A SPINNING PROJECTILE

K.H. LLOYD and D.P. BROWN

AD No. —  
DDC FILE COPY



DDC  
MAY 8 1978  
E

Approved for Public Release

UNCLASSIFIED

AR-000-966

DEPARTMENT OF DEFENCE  
DEFENCE SCIENCE AND TECHNOLOGY ORGANISATION  
WEAPONS RESEARCH ESTABLISHMENT

TECHNICAL REPORT 1906 (W)

INFLUENCE OF GRAVITY AND APPLIED SIDE FORCES ON THE  
STABILITY OF A SPINNING PROJECTILE

K.H. Lloyd and D.P. Brown

S U M M A R Y

The non-linear equations of motion of a spinning projectile are linearised by a method different from that traditionally used. This results in extra terms being retained, giving a more complete description of the shell behaviour and revealing some new information on stability. The resulting equations are solved as an eigenvalue problem, since this method of solution is the least tortuous and produces a good insight into the dynamic behaviour of the shell. It is found that the stability of the precessional and nutational modes is influenced by gravity and applied side forces. Results of numerical simulations which confirm these conclusions are given.

Approved for Public Release

---

POSTAL ADDRESS: The Director, Weapons Research Establishment,  
Box 2151, G.P.O., Adelaide, South Australia, 5001.

---

UNCLASSIFIED

DOCUMENT CONTROL DATA SHEET

Security classification of this page

UNCLASSIFIED

1 DOCUMENT NUMBERS

AR Number: AR-000-966

Report Number: <sup>14</sup> WRE-TR-1906(W) ✓

Other Numbers:

2 SECURITY CLASSIFICATION

a. Complete Document: Unclassified

b. Title in Isolation: Unclassified

c. Summary in Isolation: Unclassified

3 TITLE

<sup>6</sup> INFLUENCE OF GRAVITY AND APPLIED SIDE FORCES ON THE STABILITY OF A SPINNING PROJECTILE

4 PERSONAL AUTHOR(S):

<sup>14</sup> K.H. Lloyd D.P. Brown

<sup>9</sup> Technical rept.

5 DOCUMENT DATE:

<sup>11</sup> Nov 77

6 6.1 TOTAL NUMBER OF PAGES 28 <sup>12</sup> 24 p.

6.2 NUMBER OF REFERENCES: 5

7 7.1 CORPORATE AUTHOR(S):

Weapons Research Establishment

7.2 DOCUMENT (WING) SERIES AND NUMBER

Weapons Research and Development Wing TR-1906

8 REFERENCE NUMBERS

a. Task:

b. Sponsoring Agency:

9 COST CODE:

10 IMPRINT (Publishing establishment):

Weapons Research Establishment

11 COMPUTER PROGRAM(S) (Title(s) and language(s))

12 RELEASE LIMITATIONS (of the document):

Approved for Public Release

12.0	OVERSEAS	NO	P.R.	1	A	B	C	D	E
------	----------	----	------	---	---	---	---	---	---

Security classification of this page:

UNCLASSIFIED

371 700

13 ANNOUNCEMENT LIMITATIONS (of the information on these pages):

No limitation

14 DESCRIPTORS:

a. EJC Thesaurus Terms  
 Projectiles  
 Stability  
 Ballistics  
 Eigenvalues

b. Non-Thesaurus Terms

15 COSATI CODES:

1901  
 1407  
 1201  
 1904

16 LIBRARY LOCATION CODES (for libraries listed in the distribution):

SW SR SD AACA

17 SUMMARY OR ABSTRACT:

(if this is security classified, the announcement of this report will be similarly classified)

The non-linear equations of motion of a spinning projectile are linearised by a method different from that traditionally used. This results in extra terms being retained, giving a more complete description of the shell behaviour and revealing some new information on stability. The resulting equations are solved as an eigenvalue problem, since this method of solution is the least tortuous and produces a good insight into the dynamic behaviour of the shell. It is found that the stability of the precessional and nutational modes is influenced by gravity and applied side forces. Results of numerical simulations which confirm these conclusions are given.

ACCESSION for	
NTIS	Write Section <input checked="" type="checkbox"/>
DDC	Buff Section <input type="checkbox"/>
UNANNOUNCED	<input type="checkbox"/>
JUSTIFICATION.....	
BY.....	
DISTRIBUTION/AVAILABILITY CODES	
Dist.	AVAIL. and/or SPECIAL
A	

## TABLE OF CONTENTS

	Page No.
1. INTRODUCTION	1
2. EQUATIONS OF MOTION	2 - 3
3. SOLUTION BY EIGENVECTORS	3 - 6
4. STABILITY CRITERIA	6 - 9
5. NUMERICAL COMPUTATIONS	9 - 10
6. SUMMARY	10
7. ACKNOWLEDGEMENT	10
NOTATION	11 - 12
REFERENCES	13

## LIST OF TABLES

1. COEFFICIENTS OF EIGENVALUE EQUATION (11)	14
2. TYPICAL VALUES FOR PARAMETERS	15
3. EFFECT OF FORCES ON NORMAL MODES	15

## LIST OF FIGURES

1. Axes systems
2. Comparison of analytic solution with numerical simulation
3. Numerical simulation of motion of spinning projectile - no horizontal side forces
4. Numerical simulation of motion of spinning projectile - horizontal side force to right
5. Numerical simulation of motion of spinning projectile - horizontal side force to left

## 1. INTRODUCTION

In recent digital computer simulations of the flight of terminally guided spinning projectiles it was observed that lateral control forces sometimes lead to precessional instability. Since this result is not predicted by the traditional linear theory of shell stability, and to verify that it was not simply caused by an incorrect numerical procedure, we have re-examined the shell stability theory. It turns out the result is predictable by a linear theory provided that the exact equations of motion are expressed in the nonspinning axes system ( $p_a = 0$ ) before linearisation.

Nicholaides(ref.1) and Murphy(ref.2) have contributed significantly to the study of the stability of spinning projectiles, and their results are still those most frequently quoted today. Both these workers linearised the equations of motion, but they also assumed that the flight path was almost horizontal in order to further simplify the equations. This meant that the effects of gravity and applied side forces produced, for example, by canards (Regan and Smith, reference 3) did not enter into their criteria for stability. It is because we are here concerned with quite large side forces, comparable with the projectile's weight, that the usual approximations become inadequate.

By expressing the equations of motion in nonspinning axes and then linearising, but without assuming that the flight path elevation angle is small, we obtain a system of six first order ordinary differential equations, the solution of which reveals the influence of gravity and side forces on stability.

The equations are solved as an eigenvalue problem. This elegant technique, which does not appear to have been used in shell stability problems previously, yields expressions for nutational and precessional damping rates and frequencies (these being the eigenvalues) very readily. The linearisation procedure gives two more equations than the usual treatment does (relating to the Euler roll angle  $\varphi$ , and the elevation  $\theta$ , of the non-spinning axes) which introduces another mode of motion which we shall call the  $\theta, \varphi$  mode. It will be shown that this mode represents the curvature of the trajectory.

In the next section we present the equations of motion, first in the so-called aeroballistic axes and then transformed to nonspinning axes. We have not used distance along the trajectory as the independent variable, as is often done. This means that the effect of drag on stability is neglected; but its effect is small, and retaining time as the independent variable simplifies the present analysis. A wish to refrain from needlessly complicating the treatment with terms which produce negligible effect on stability has also resulted in our excluding Magnus force (however, Magnus moment cannot be neglected). The effects of the neglected terms are adequately discussed in reference 1.

Section 3 solves the linearised equations of motion as an eigenvalue problem and Section 4 evaluates the stability criteria from the derived eigenvalues. It is found that the motion of a typical 105 mm shell remains stable provided the horizontal component of the control force, when applied at the nose, remains less than about 50 N. For larger side forces either nutational or precessional instability may be produced depending upon the trajectory elevation angle and whether the force is towards the right or left of the trajectory. On the down-leg, for example, assuming that the shell spin is clockwise when viewed from the rear, a horizontal force to the right, applied at the nose, tends to stabilise precession and destabilise nutation, while a force to the left tends to destabilise precession and stabilise nutation. The opposite occurs on the up-leg or if the sense of shell rotation is reversed, and the effect diminishes as the trajectory elevation angle approaches zero. Instability with vertical control forces, applied at the nose, does not occur until the force exceeds about 1000 N. The effect of gravity on stability is very small.

Finally, Section 5 gives results of numerical solutions of the equations of motion. These agree fairly well with the analytic solution.

## 2. EQUATIONS OF MOTION

The axes systems used in formulating the problem are illustrated in figure 1. In addition to the standard aerodynamic forces and gravity, the spinning projectile is also subjected to a lateral control force, applied at the nose, normal to its axis, with components E and F as indicated in figure 1. Such a force could be applied, for example, by canards mounted on the nose, the nose being mechanically decoupled in roll from the projectile and roll stabilised relative to earth. The equations of motion will first be written in aeroballistic axes, the angular velocity of which is  $(p_a, q, r)$  with  $p_a = -r \tan \theta$ ;  $p_a$  is the roll rate

necessary to keep the y axis horizontal. The x axis lies along the projectile spin axis, y lies to the right in a horizontal plane, and z in a vertical plane. These axes are often preferred because they represent quantities in a way which is easily understood by a ground based observer.

Neglecting changes in spin rate and axial velocity, which are small and inconsequential to our problem, assuming small incidence, and putting  $u = v$ , the equations of motion are (see, for example, Kolk, reference 4):

$$\dot{v} = Z_w v - Vr - r \tan \theta \cdot \dot{w} + E/m \quad (1)$$

$$\dot{w} = Z_w w + Vq + r \tan \theta \cdot v + g \cos \theta + F/m \quad (2)$$

$$\dot{q} = N_{pw} v + M_w w + M_q q - (pA/B) r - r \tan \theta \cdot r - XF/B \quad (3)$$

$$\dot{r} = -M_w v + N_{pw} w + (pA/B) q + M_q r + r \tan \theta \cdot q + XE/B \quad (4)$$

where the aerodynamic force and moment derivatives are given by:

$$M_w = \frac{1}{2} \rho V^2 Sd \cdot C_{m\alpha} / BV$$

$$Z_w = \frac{1}{2} \rho V^2 S \cdot C_{N\alpha} / mV$$

$$M_q = \frac{1}{2} \rho V^2 Sd \cdot (qd/2V) \cdot C_{mq} / Bq$$

$$N_{pw} = \frac{1}{2} \rho V^2 Sd \cdot (pd/2V) \cdot C_{np\alpha} / BV$$

Because of the factors  $(r \tan \theta)$  and  $\cos \theta$ , equations (1) to (4) are non-linear. The terms involving  $r \tan \theta$  are small, and a linearisation which neglects them is usually a good approximation, particularly if the flight path elevation  $\theta$  is small. However, by making this approximation, one obtains a solution whose stability does not depend on the applied forces and gravity, contrary to our numerical experiences. Neglecting the terms containing  $(r \tan \theta)$  is equivalent to neglecting the residual roll rate ( $p_a = -r \tan \theta$ ) which is necessary to keep the y axis of the aeroballistic axes horizontal as the projectile pitches and yaws. These linearised equations therefore in fact refer strictly to the nonspinning axes ( $p_a = 0$ ), but they incorrectly imply that E, F and g act in a constant direction in this axes system. We shall now show that if one starts with the exact equations of motion in nonspinning axes and then linearises them, one obtains a set of equations which, to first order, correctly allow for the variation in the direction of E, F and g in these axes.

Transforming equations (1) to (4) into the nonspinning axes system is effected by rotation about the x axis by the angle  $\varphi$ , where  $\varphi = \int (r \cos \theta + q \sin \theta) \tan \theta dt$  is the change of Euler roll angle suffered by the nonspinning axes.

The transformation gives:

$$\dot{v} = Z_w v - Vr + (g \cos \theta_0 + F/m) \varphi + E/m \quad (5)$$

$$\dot{w} = Z_w w + Vq - (E/m) \varphi - (g \sin \theta_0) \theta + (g \cos \theta_0 + F/m) \quad (6)$$

$$\dot{q} = N_{pw} v + M_w w + M_q q - (pA/B) r + (XE/B) \varphi - XF/B \quad (7)$$

$$\dot{r} = -M_w v + N_{pw} w + (pA/B) q + M_q r + (XF/B) \varphi + XE/B. \quad (8)$$

To complete this set of equations we need a pair of equations giving the rates of change of  $\theta$  and  $\varphi$ . These are given to first order by:

$$\dot{\theta} = q \quad (9)$$

$$\dot{\varphi} = r \tan \theta_0 \quad (10)$$

Note that the variables are now with respect to the nonspinning axes. In deriving equations (5) to (10) we have assumed  $\varphi$  is small, so have put  $\cos \varphi = 1$ ,  $\sin \varphi = \varphi$ , and have neglected products such as  $r\varphi$  and  $q\varphi$ . The validity of this assumption will be discussed later. Note that there is no loss of generality in assuming that  $\varphi = 0$  initially. We have also assumed that the interval being considered is sufficiently short that variations in  $\theta$  are small, thereby replacing  $\theta$  by  $(\theta_0 + \theta)$ , where  $\theta$  is now the departure from its initial value,  $\theta_0$ ; this restricts the time interval to a few seconds.

It should be observed in the above that the linearisation of the transformed equations is not equivalent to the transformation of the linearised equations; ignoring the  $r \tan \theta$  terms in equations (1) to (4) has no equivalent in equations (5) to (10). Although the  $r \tan \theta$  terms are second order in magnitude, it will be seen that their cumulative influence upon the stability of the solutions is sometimes comparable to that of the first order pitch damping terms. This is a rather sobering example of the fact that when nonlinear equations are simplified, the relative numerical size of a term is not the sole criterion determining its importance.

### 3. SOLUTION BY EIGENVECTORS

Equations (5) to (10) give 6 linear first order equations in six unknowns  $v$ ,  $w$ ,  $q$ ,  $r$ ,  $\varphi$  and  $\theta$ . These can be written in matrix form as

$$\dot{\bar{x}} = \bar{M} \bar{x} + \bar{N}.$$

To determine the stability of the solution of this set of equations, we examine the general solution of the homogeneous equation

$$\dot{\bar{x}} = \bar{M} \bar{x}.$$

Following Struble(ref.5) we consider the linear transformation,  $\bar{u} = \bar{U} \bar{x}$ , where  $u_i$  are the eigenvectors of the matrix  $\bar{M}$ . The eigenvectors satisfy the six independent equations

$$\dot{u}_i = \psi_i u_i, \quad i = 1, 6$$

with the solutions  $u_i = u_{i0} \exp(\psi_i t)$ , where  $\psi_i$  are the eigenvalues of the matrix  $\bar{M}$ . They satisfy the equation

$$|\bar{M} - \psi \bar{I}| = 0,$$

where  $\bar{I}$  is the diagonal identity matrix.

Using the values for the elements of  $M$  given by equations (5) to (10), and expanding the determinant gives a sixth degree polynomial equation for  $\psi$ :

$$\psi^6 + a_1 \psi^5 + a_2 \psi^4 + a_3 \psi^3 + a_4 \psi^2 + a_5 \psi + a_6 = 0 \quad (11)$$

where

$$a_1 = -2(m_q + Z_w)$$

$$a_2 = (pA/B)^2 + 2(M_q Z_w - M_w V) + (M_q + Z_w)^2 - XF \tan \theta_o / B$$

$$a_6 = \{(M_w^2 + N_{pw}^2)(g \cos \theta_o + F/m) - (N_{pw} E - FM_w) Z_w X/B\} g \sin \theta_o \cdot \tan \theta_o.$$

The other coefficients all have terms involving  $E$ ,  $F$ ,  $g$ ,  $XE$  and  $XF$ , so it is simplest to present them in tabular form, which is done in Table 1. For each entry in the table, the dominant component is given first.

As an aside, it is interesting to note that for no external forces the eigenvalue equation factorises into:

$$\psi^2 - [Z_w + M_q + ipA/B] \psi + [Z_w M_q - VM_w] + i[Z_w pA/B - VN_{pw}] = 0 \quad (12)$$

and a similar equation with  $i$  replaced by  $-i$ , i.e. its complex conjugate; only the roots of equation (12) are physically admissible. The two equations give roots which are complex conjugates of each other. Note that equation (12) is basically the same as the equation Murphy uses in his discussion of projectile stability(ref.2).

Returning to equation (11), the coefficients of the terms in the eigenvalue equation are quite complicated. Fortunately for a typical spinning projectile a few of the terms dominate and the others may be neglected.

In Table 2 we have listed representative values for all the parameters in our problem. Using these values to determine the dominant terms, we obtain the following simplified expressions for the coefficients of equation (11):

$$a_1 = -2(M_q + Z_w) \quad (13)$$

$$a_2 = (pA/B)^2 - 2VM_w \quad (14)$$

$$a_3 = -2(pA/B)(Z_w pA/B - VN_{pw}) + 2VM_w(M_q + Z_w) - X(pA/B^2)E \tan \theta_0 \quad (15)$$

$$a_4 = V^2 M_w^2 \quad (16)$$

$$a_5 = -2VM_w^2 \cdot g \sin \theta_0 - (g \sin \theta_0 + VZ_w)(M_w X/B)F \tan \theta_0 \quad (17)$$

$$a_6 = M_w^2 \cdot g^2 \sin^2 \theta_0 + (M_w + Z_w X m/B)(M_w/m)g \sin \theta_0 \cdot F \tan \theta_0 \quad (18)$$

Although interest is centered on the eigenvalues, for it is they that determine stability, we will briefly discuss the eigenvectors. They are given by the solutions of the equations from which the eigenvalue determinant is extracted. Since there are four unknowns and four equations, it is necessary to express three of the variables as a function of the fourth. In order to compare the magnitudes of the eigenvectors, the eigenvectors need to be in the same units; so we will introduce the dimensionless variables (all of them angles):

$$\begin{aligned} \alpha_e &= w_e/V, \beta_e = v_e/V \\ \eta_e &= q_e/\psi, \zeta_e = r_e/\psi \end{aligned}$$

where the subscript e denotes that these are the eigenvectors. Solving the equations in terms of these variables gives:

$$\begin{aligned} \beta_e &= -i \alpha_e \\ \eta_e &= i[Z_w/\lambda - 1] \alpha_e \\ \zeta_e &= [Z_w/\lambda - 1] \alpha_e \end{aligned}$$

In order to see what these eigenvectors look like, we will anticipate the solution of the eigenvalues. It will be shown that they satisfy the inequalities  $\omega > 1 > \lambda$ , which leads to the approximations:

$$\begin{aligned} \beta_e &= -i \alpha_e \\ \eta_e &= (Z_w/\omega - i) \alpha_e \\ \zeta_e &= (-1 + iZ_w/\omega) \alpha_e \end{aligned}$$

Typical values of  $Z_w/\omega$  are 0.03 for precession and 0.0013 for nutation, from which it follows that the angular excursions of the eigenvectors are of nearly the same magnitude, and they are close to phase quadrature. When the motion is constrained to rotation about the center of gravity, i.e.,  $Z_w = 0$ , the eigenvectors are exactly in phase quadrature. It is seen that having no such constraint makes only a small difference to the eigenvectors.

Addition of gravity and side forces complicates the eigenvectors enormously. Not only are the expressions for  $\beta_e$ ,  $\eta_e$ ,  $\zeta_e$  modified, but there are, of course, two extra terms, corresponding to  $\varphi$  and  $\theta$ . However, the simple relationships

$$\theta_e = \eta_e$$

$$\varphi_e = \tan \theta_o \zeta_e$$

show that the  $\varphi$  eigenvector vanishes for horizontal flight but the  $\theta$  eigenvector does not.

#### 4. STABILITY CRITERIA

The frequency and damping of the normal modes of the projectile's motion are given by the imaginary and real parts of the eigenvalues of equation (11). Rather than attempt to attack this equation directly, we shall adopt an approach which makes use of the known properties of the solutions.

As discussed earlier, when gravity and side forces are not present, the eigenvalue equation reduces to a fourth degree one whose solution is well known, consisting of two pairs of complex conjugates. The motions corresponding to these are the precessional and nutational modes:

$$\psi_P = \lambda_P \pm i\omega_P$$

$$\psi_N = \lambda_N \pm i\omega_N$$

whose relative magnitudes for a typical spinning projectile are:

$$\omega_N \gg \omega_P > 1, \quad |\lambda|_N \sim |\lambda|_P < 1.$$

Introduction of equations (9) and (10) increases the degree of the eigenvalue equations by two and so introduces two more roots, which we shall denote by  $\psi_{\theta, \varphi}$ . These roots may either be a complex conjugate pair, or both real. For now we shall assume they are of the form

$$\psi_{\theta, \varphi} = \lambda_{\theta, \varphi} \pm i\omega_{\theta, \varphi}$$

where  $\omega_{\theta, \varphi}$  is imaginary when the roots  $\lambda_{\theta, \varphi}$  are real. The roots tend to zero for vanishingly small values of  $g \sin \theta$ ,  $E$  and  $F$ , and, as will be shown, they are always much less than unity.

Expressing the roots in this form gives a sixth degree polynomial for the eigenvalues:

$$\psi^6 + b_1 \psi^5 + b_2 \psi^4 + b_3 \psi^3 + b_4 \psi^2 + b_5 \psi + b_6 = 0 \quad (19)$$

where the coefficients are sums and products of the  $\lambda$ 's and  $\omega$ 's. By retaining only the dominant terms these simplify to

$$b_1 = -2(\lambda_P + \lambda_N + \lambda_{\theta, \varphi}) \quad (20)$$

$$b_2 = \omega_N^2 \quad (21)$$

$$b_3 = -2\omega_N^2 (\lambda_p + \lambda_{\theta,\varphi}) \quad (22)$$

$$b_4 = \omega_N^2 \omega_p^2 \quad (23)$$

$$b_5 = -2\omega_N^2 \omega_p^2 \lambda_{\theta,\varphi} \quad (24)$$

$$b_6 = \omega_N^2 \omega_p^2 (\lambda_{\theta,\varphi}^2 + \omega_{\theta,\varphi}^2) \quad (25)$$

We are now in a position to obtain explicit expressions for the eigenvalues in terms of the parameters of the problem. First we confirm that  $\lambda_{\theta,\varphi}$  and  $\omega_{\theta,\varphi}$  are indeed small; from equations (16), (17), (18), (23), (24) and (25) we have

$$\lambda_{\theta,\varphi} = g \sin \theta_o / V + (Z_w + g \sin \theta_o / V) (X/2VM_w B) F \tan \theta_o \quad (26)$$

$$\omega_{\theta,\varphi}^2 = [(M_w - X m g \sin \theta_o / BV) / (V^2 M_w m)] g \sin \theta_o \cdot F \tan \theta_o \quad (27)$$

The largest term in either of these expressions is  $g \sin \theta_o / V$ , which is of the order of 0.04.

Equations (14) and (21) give immediately for  $\omega_N$ :

$$\omega_N = pA/B - VM_w B/pA \quad (28)$$

correct to first order in the binomial expansion for the square root. We can now calculate  $\omega_p$  from equations (16) and (23):

$$\omega_p = VM_w B/pA + V^2 M_w^2 (B/pA)^3 \quad (29)$$

Also, from equations (13), (15), (20), (22) we have:

$$\begin{aligned} \lambda_N = & M_q + [1 + 2VM_w (B/pA)^2] VN_{pw} B/pA \\ & + (M_q - Z_w) (B/pA)^2 VM_w - (X/2pA) [1 + 2VM_w (B/pA)^2] E \tan \theta_o. \end{aligned} \quad (30)$$

Finally, from equations (15) and (22):

$$\begin{aligned} \lambda_p = & Z_w - [1 + 2VM_w (B/pA)^2] VN_{pw} B/pA \\ & - (M_q - Z_w) (B/pA)^2 VM_w + (X/2pA) [1 + 2VM_w (B/pA)^2] E \tan \theta_o \\ & - g \sin \theta_o / V - (Z_w + g \sin \theta_o / V) (X/2VM_w B) F \tan \theta_o. \end{aligned} \quad (31)$$

In every case we have put the dominant terms first in the expressions on the right hand side. When  $E = F = g = 0$  these expressions reduce to the well known solutions of the linearised equations of motion (ref.1). Pitch damping and normal force are the prime stabilising factors for nutation and precession respectively.

If the Magnus moment is large, one or other of precession and nutation becomes unstable. The precessional and nutational frequencies are seen to be independent of gravity and side forces to second order, whereas the damping depends on these forces to the first order of approximation. However, the terms involving the vertical applied force,  $F$ , are generally much smaller than those involving the horizontal force,  $E$ . For the time being, therefore, we shall neglect the terms in  $F$ .

A given mode is unstable if the corresponding  $\lambda$  is positive. From the sign of each term in the expressions for  $\lambda$  we can ascertain whether given forces are stabilising or destabilising. This information is summarised in Table 3. For both nutation and precession, the destabilising force must be greater than a certain minimum value to overcome the stabilising influence of  $M_q$  and  $Z_w$  respectively.

Substituting values for the parameters listed in Table 2 gives the following approximate expressions for the eigenvalues:

$$\omega_p = 4.5 \text{ rad s}^{-1}$$

$$\lambda_p = -0.269 + 0.0067 E \tan \theta_o - 0.039 \sin \theta_o \text{ s}^{-1}$$

$$\omega_N = 105 \text{ rad s}^{-1}$$

$$\lambda_N = -0.353 - 0.0067 E \tan \theta_o \text{ s}^{-1}.$$

The contribution of the vertical force,  $F$ , has again been omitted as it is smaller than the other terms.

We have plotted damping rates,  $\lambda$ , in figure 2. It is seen that the projectile is nutationally unstable for  $E \tan \theta < -60N$ , and precessionally unstable for  $E \tan \theta > 40N$ .

The  $\theta, \varphi$  mode is a mode of motion which arises from the introduction of equations (9) and (10), which allows  $\theta$  and  $\varphi$  to vary. Note that this mode has a time constant of the order to 25 s and so does not vary significantly during the few seconds of validity of the solution. Its physical significance is that it represents the curvature of the trajectory. We shall demonstrate this for the case where gravity is the only external force.

First, let  $\epsilon$  be the elevation of the tangent to the trajectory. By relating its rate of change to the force normal to the trajectory we have

$$d\epsilon/dt = -g \cos \epsilon / V.$$

Now  $\epsilon = \theta - a$ , where  $a$  is the vertical component of incidence, positive when the shell nose is above the tangent to the flight path. Replacing  $\theta$  by  $\theta_o + \theta$ , expanding  $\cos(\theta - a)$ , and using the small angle approximations  $\sin a = a$ ,  $\sin \theta = \theta$ , gives

$$d(\theta - a)/dt = (g \sin \theta_o / V) (\theta - a) - g \cos \theta_o / V$$

The general solution of this equation has a time constant  $V/g \sin \theta_o$ , which is the same as for the eigenvalue for the  $\theta, \varphi$  mode.

Second, since, from equation (5),

$$r \sim (g \cos \theta_o / V) \varphi + \dots$$

it follows from equation (10) that

$$\dot{\phi} \sim (g \sin \theta_0 / V) \phi + \dots,$$

the solution of which also has the time constant  $V/g \sin \theta_0$ .

This confirms our interpretation of the  $\theta, \varphi$  mode. The degeneracy of the roots of the  $\theta, \varphi$  mode is removed by the normal force, F. The form of the roots of the  $\theta, \varphi$  mode depends on the sign of  $\omega^2_{\theta, \varphi}$ , given by equation (27). Since  $|M_w - Xmg \sin \theta_0 / BV|$  is positive for the parameter values given in Table 2, the sign of  $\omega^2_{\theta, \varphi}$  is then the same as the sign of F. For F positive, i.e. downward force, the two eigenvalues are a pair of complex conjugate numbers. For F negative, we put  $\Delta\lambda^2 = -\omega^2_{\theta, \varphi}$ , and the eigenvalues have the real values,  $\lambda \pm \Delta\lambda$ .

### 5. NUMERICAL COMPUTATIONS

There is always satisfaction when exact numerical calculations confirm an analytic treatment. This, plus the benefit of computer plotted figures showing the nutational and precessional instabilities very clearly, are our excuses for presenting the results of some numerical simulations in this section.

We have written a 6 degree of freedom computer program to calculate the projectile motion numerically. The equations solved are (1) to (4) plus the equations of motion in the x direction:

$$\begin{aligned} \dot{u} &= \frac{1}{2} \rho V^2 S C_x - qw + rv - g \sin \theta \\ \dot{p} &= \frac{1}{2} \rho V^2 S C_{lp} \cdot pd / 2V \end{aligned}$$

with  $C_x = -0.13$  and  $C_{lp} = -0.025$ . We have also added a Magnus force term to equations (1) and (2), with  $C_{Ypa} = -1.5$ . By running the program with and without these refinements, the contribution of these added refinements was found to be small, but they have been added for completeness.

The results of three runs of the program are given in figures 3 to 5. The shell parameters were set at the values given in Table 2, which apply to halfway down the downleg of a typical 105 mm shell trajectory. The elevation was set initially at  $-43^\circ$  and the velocity at  $250 \text{ ms}^{-1}$ . During the 4 s for which the trajectory was calculated the mean elevation decreased to  $-48^\circ$  and the velocity increased to  $264 \text{ ms}^{-1}$ ; i.e. these values did not depart too much from the constant value assumed in the analytic solution. The numerical calculations used a standard fourth order Runge-Kutta routine. The time step was 0.0025 s; if it was much larger than this nutation was found to be artificially damped.

Each figure shows the incidence ( $\beta, \alpha$ ) and the angular rate ( $q, r$ ); it also shows values of  $\dot{\phi}$  and its integral  $\varphi$ , the Euler roll angle of the nonspinning axes, as functions of time. These figures show very clearly the conditions for instability which were discovered analytically. With no side forces acting (figure 3), both precessional and nutational modes are stable; a 100 N force to the right (figure 4) produces nutational instability and increases the precessional stability, whereas a 50 N force to the left (figure 5) gives precessional instability while increasing nutational stability.

The precessional and nutational modes are easily distinguished in figures 3 to 5, so estimates can be made of their frequency and damping. The results are also plotted in figure 2. Comparison with the eigenvalues of the analytic treatment shows a systematic difference in  $\lambda$  of about  $0.01 \text{ s}^{-1}$ , due to the neglect of drag in the analytic treatment. Murphy (ref.2) has shown that drag has a destabilising effect, increasing  $\lambda$  by  $\frac{1}{2} \rho V^2 S C_D / mV$ . For the case we are considering here, this equals  $0.01 \text{ s}^{-1}$ . In addition to the systematic difference, there is a scatter of about  $0.005 \text{ s}^{-1}$ , which is largely due to errors in estimating  $\lambda$  from the numerical simulations.

Finally, the numerical calculations enable us to see how valid was our assumption that the integrated residual roll,  $\varphi$ , was small. It is seen that although  $\varphi$  is very small ( $\sim 0.01$  rad) when there are no side forces, the approximation is only valid on short time intervals for large side forces, where  $\varphi$  can approach 1 rad after a few seconds.

## 6. SUMMARY

The equations of motion of a spinning projectile have been written in non-spinning axes, whose angular velocity is  $(0, q, r)$ , in which the directions of gravity and side forces are not constant, but wobble in the complementary manner to the Eulerian roll angle of the nonspinning axes system. By assuming that this wobble is small, an analytic solution of the linearised equations is obtained whose general solution contains gravity and side forces in the damping term.

It is found that on the trajectory downleg, a horizontal side force to the right, applied at the nose, tends to stabilise precession and destabilise nutation, and a force to the left tends to destabilise precession and stabilise nutation. The opposite occurs on the upleg. This means that a large enough side force (greater than about 40 N, for a 105 mm shell, when applied at the nose) will always cause the motion of the projectile to be unstable.

Gravity, and side forces in the vertical plane, have a much smaller effect on precessional and nutational stability than do horizontal side forces. For expected parameter values, these forces are unlikely to be large enough to overcome the stabilising effect of the aerodynamic damping moment and normal force.

Numerical simulation of the motion of a projectile using a 6 degree of freedom computer program has confirmed these predictions of the analysis.

## 7. ACKNOWLEDGEMENT

We wish to thank Dr R.L. Pope of Dynamics Group, Aerospace Division, for the many fruitful discussions we had together.

## NOTATION

$a_i$	coefficients in eigenvalue polynomial equation
A	moment of inertia about x axis
$b_i$	coefficients in eigenvalue equation in terms of roots
B	moment of inertia about y and z axes
$C_{lp}$	roll damping moment coefficient derivative
$C_{ma}$	pitching moment coefficient derivative
$C_{mq}$	pitch damping moment coefficient derivative
$C_{Na}$	normal force coefficient derivative
$C_{npa}$	Magnus moment coefficient derivative
$C_x$	axial force coefficient
$C_{Ypa}$	Magnus force coefficient
d	reference length ( $\equiv$ projectile diameter)
E	applied side force in horizontal direction
F	applied side force in vertical direction
g	gravitational constant
$\bar{I}$	identity matrix
m	mass
$\bar{M}, \bar{N}, \bar{U}$	matrices in Section 3
$M_w$	pitching moment derivative (equation (3))
$M_q$	pitch damping moment derivative (equation (3))
$N_{pw}$	Magnus moment derivative (equation (3))
p	projectile roll rate
$p_a$	roll rate of axes system $\begin{cases} = -r \tan \theta & \text{in aeroballistic axes} \\ = 0 & \text{in nonspinning axes} \end{cases}$
q	angular velocity about y axis
r	angular velocity about z axis
S	reference area ( $= \pi d^2 / 4$ )
t	time
$u_i$	eigenvector of motion
u	velocity component in x direction

$v$	velocity component in y direction	
$V$	projectile velocity (in still air)	
$w$	velocity component in z direction	
$\bar{x}$	vector ( $v, w, q, r, \varphi, \theta$ )	
$x$	along projectile	} aeroballistic axes
$y$	horizontal	
$z$	in vertical plane	
$X$	distance of side force forward from c.g.	
$Z_w$	normal force derivative (equation (1))	
Greek letters		
$\alpha$	vertical component of incidence, positive nose up	
$\epsilon$	elevation of tangent to trajectory	
$\lambda$	damping (real part of eigenvalue)	
$\theta$	elevation of the x axis	
$\theta_0$	initial elevation	
$\rho$	atmospheric density	
$\varphi$	residual roll angle of nonspinning axes ( $= -\int r \tan \theta dt$ )	
$\psi$	eigenvalues of motion	
$\omega$	frequency (imaginary part of eigenvalue)	

## Subscripts and superscripts

$N$	nutational mode
$P$	precessional mode
$\theta, \varphi$	$\theta, \varphi$ mode
$\dot{\phantom{a}}$	differentiation with respect to time
$\bar{A}, \bar{a}$	matrix or vector

REFERENCES

No.	Author	Title
1	Nicolaides, J.D.	"Free Flight Dynamics". Department of Aerospace Engineering, University of Notre Dame. c 1968
2	Murphy, C.H.	"Free flight motion of Symmetric missiles". Ballistic Research Laboratories, Rept. 1216 Aberdeen Proving Ground, Maryland, 1963
3	Regan, F.J. and Smith, J.	"Aeroballistics of a terminally corrected spinning projectile". J. Spacecraft <u>12</u> , 733, 1975
4	Kolk, W.R.	"Modern Flight Dynamics". Prentice Hall Pub. Co. 1961
5	Struble, R.A.	"Nonlinear differential equations". McGraw Hill Book Co. 1962

TABLE 1. COEFFICIENTS OF EIGENVALUE EQUATION (11)

Coefficients Multiplies	$a_3$	$a_4$	$a_5$
1	$-2(Z_w p_A/B - N_{pw} V) p_A/B$ $-2(M_q + Z_w)(M_q Z_w - VM_w)$	$(M_q Z_w - M_w V)^2$ $+ (Z_w p_A/B - N_{pw} V)^2$	-
$E \tan \theta_o / m$	$N_{pw}$	$M_w p_A/B - N_{pw} (M_q + Z_w)$	$-Z_w (M_w p_A/B - N_{pw} M_q)$
$XE \tan \theta_o / B$	$-p_A/B$	$2Z_w p_A/B - N_{pw} V$	$-Z_w (Z_w p_A/B - N_{pw} V)$
$F \tan \theta_o / m$	$M_w$	$-M_w (M_q + Z_w) - N_{pw} p_A/B$	$-V(M_w^2 + N_{pw}^2)$ $+ Z_w (N_{pw} p_A/B + M_w M_q)$
$XF \tan \theta_o / B$	$M_q + 2Z_w$	$-M_w V - Z_w (M_q + 2Z_w)$	$-Z_w (VM_w - M_q Z_w)$
$g \sin \theta_o$	$2M_w$	$-2M_w (M_q + Z_w) - 2N_{pw} p_A/B$	$-2V(M_w^2 + N_{pw}^2)$ $+ 2Z_w (N_{pw} p_A/B + M_w M_q)$
$g \sin \theta_o \tan \theta_o$	-	-	$(N_{pw} E - M_w F) X/B$

TABLE 2. TYPICAL VALUES FOR PARAMETERS

Primary parameters		Derived parameters	
V	250 m.s <sup>-1</sup>		
p	1050 rad.s <sup>-1</sup>		
ρ	1.05 kg.m <sup>-3</sup>		
m	15 kg		
A	0.023 kg.m <sup>2</sup>		
B	0.22 kg.m <sup>2</sup>		
d	0.105 m	S	0.0087 m <sup>2</sup>
X	0.3 m		
C <sub>ma</sub>	3.8	M	2.07 m <sup>-1</sup> .s <sup>-1</sup>
C <sub>Na</sub>	-1.8	Z <sub>w</sub>	-0.137 s <sup>-1</sup>
C <sub>mq</sub>	-16	M <sub>q</sub>	-0.457 s <sup>-1</sup>
C <sub>npa</sub>	0.4*	N <sub>pw</sub>	0.048 m <sup>-1</sup> .s <sup>-1</sup>
E	0 → 100 N <sup>+</sup>		
F	0 → 100 N <sup>+</sup>		
g	9.8 m.s <sup>-2</sup>		

The values apply to halfway on the downleg of a 105 mm shell trajectory.

\* Magnus moment increases rapidly from 0.02 to 1.0 in the transonic region. We have taken a mean value.

+ Canards mounted on the nose are likely to produce side forces in this range.

TABLE 3. EFFECT OF FORCES ON NORMAL MODES

Force	Precession	Nutation
g sin θ > 0	stabilising	nil
< 0	destabilising	nil
E tan θ > 0	destabilising	stabilising
< 0	stabilising	destabilising
F tan θ > 0	stabilising	nil
< 0	destabilising	nil

θ is positive on the upleg

E is positive to the right viewed from the rear

F is positive downwards

Projectile spins clockwise as viewed from rear

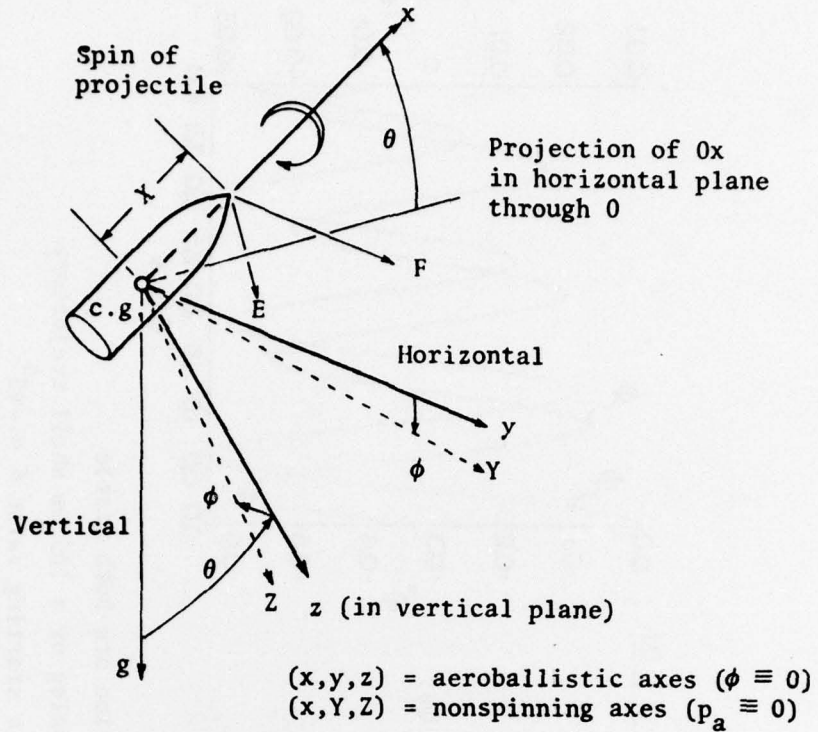
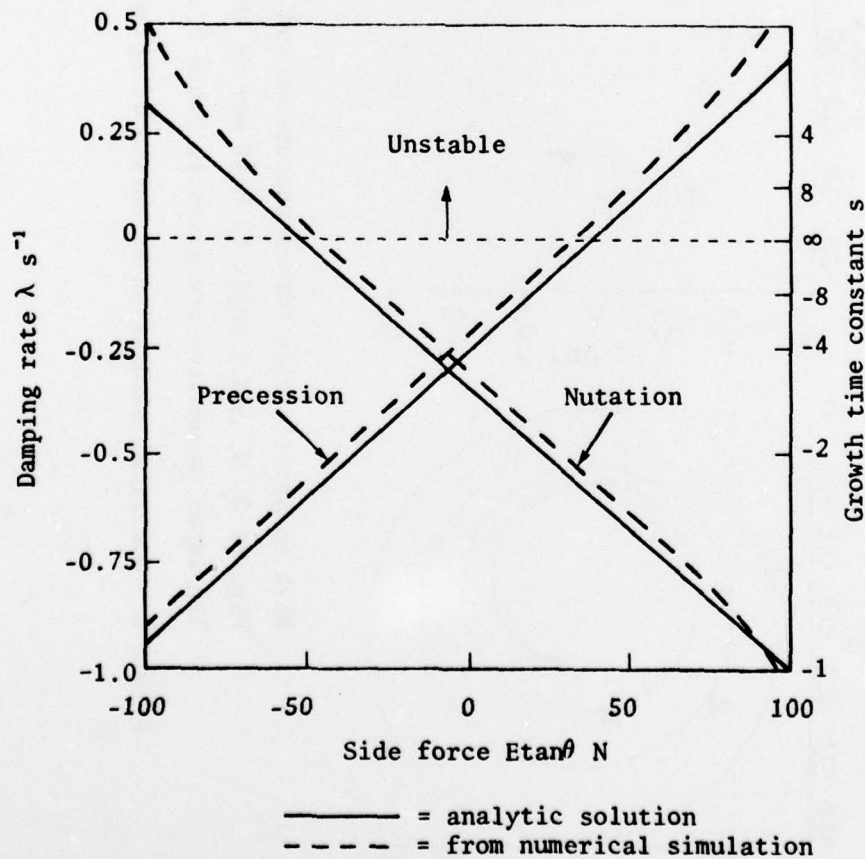
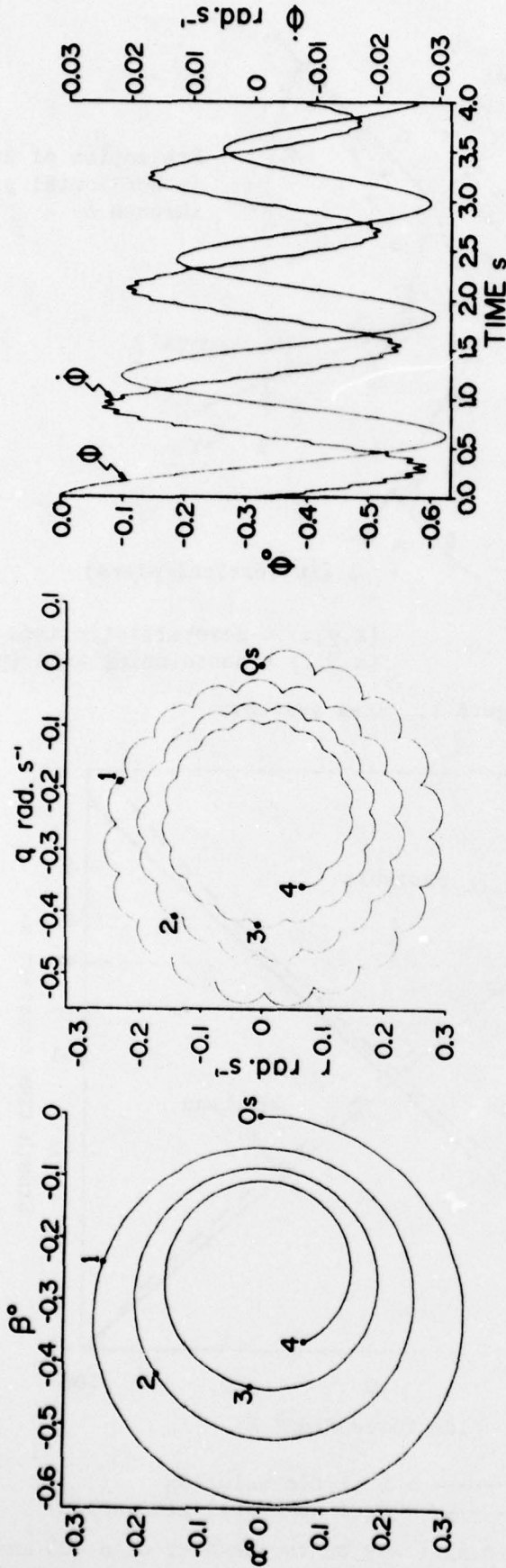


Figure 1. Axes systems



These calculations apply to half way on the downleg of a 105 mm shell trajectory.

Figure 2. Comparison of analytic solution with numerical simulation

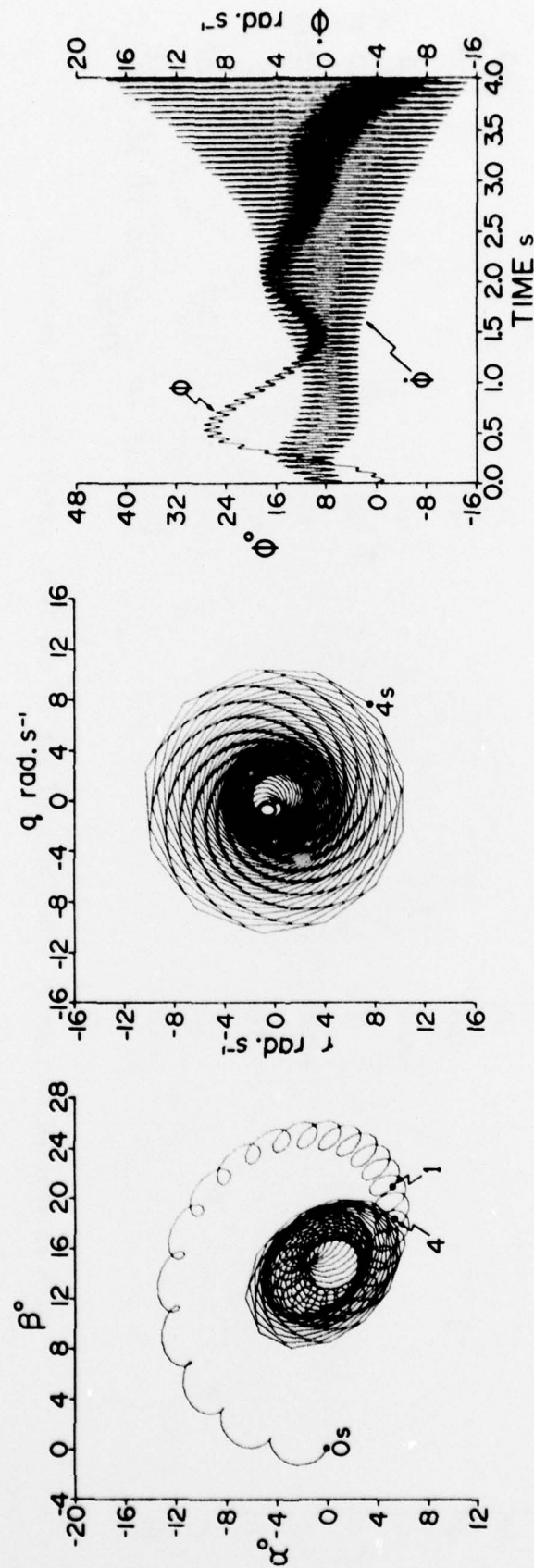


With no applied side forces precession and nutation are both stable

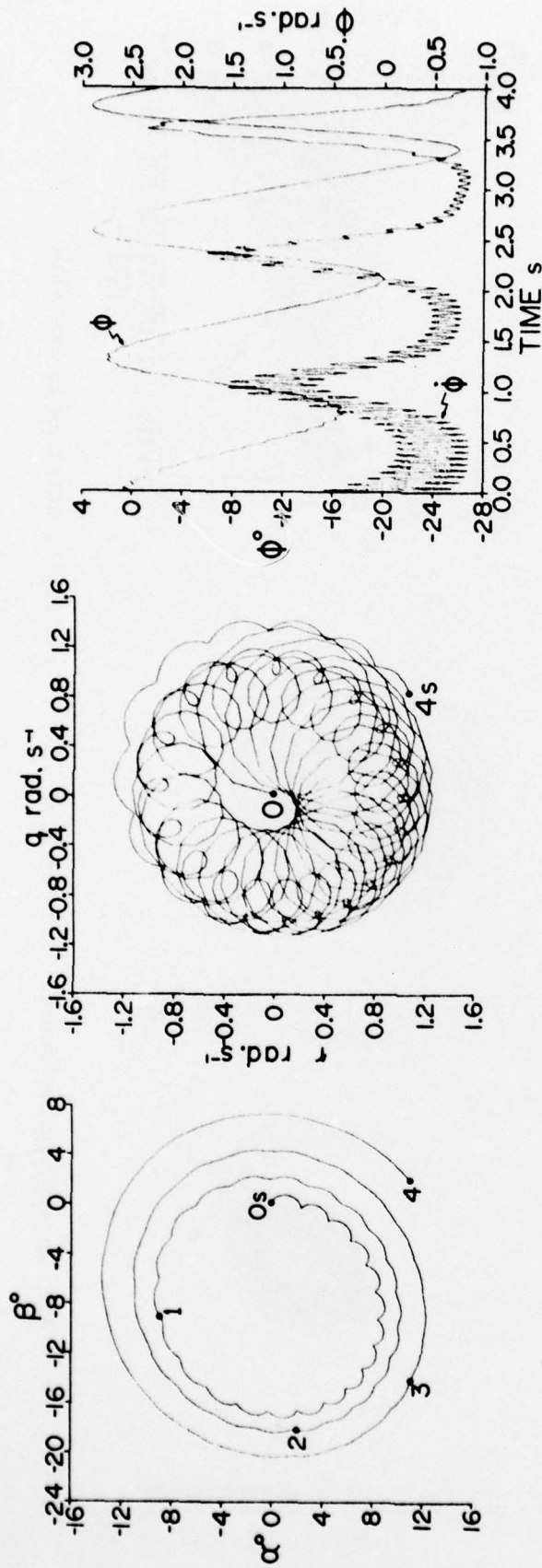
Figures 3, 4, and 5 apply to half way on the downleg of a 105 mm shell trajectory

The input parameters are given in Table 2, with a starting value  $\theta = -43^\circ$

Figure 3. Numerical simulation of motion of spinning projectile - no horizontal side forces



With an applied horizontal side force of 100N to the right, nutation is unstable  
Figure 4. Numerical simulation of motion of spinning projectile - horizontal side force to right



With an applied horizontal side force of 50N to the left, precession is unstable

Figure 5. Numerical simulation of motion of spinning projectile - horizontal side force to left

## DISTRIBUTION

Copy No.

## EXTERNAL

## In United Kingdom

Defence Scientific and Technical Representative, London	1
Defence Research and Development Representative, London	2
R.A.E., Aero Department	3 - 4
Space Department	5
Weapons Department	6 - 7
Bedford	8
Library	9
R.A.R.D.E.	10
T.T.C.P., U.K. National Leader Panel W-2	11 - 14
Aeronautical Research Council	15 - 16
Aircraft Research Association (Bedford)	17
C.A.A.R.C. Secretary	18
National Lending Library of Science and Technology	19
Royal Aeronautical Society, Library	20

## In United States of America

Counsellor, Defence Science, Washington	21
Defence Research and Development Attache, Washington	22
Air Force Armament Testing Laboratory	23
Ballistics Research Laboratories	24
Edgewood Arsenal	25
Eglin Air Force Base	26
N.A.S.A.	27 - 30
Naval Surface Weapons Center	
Dahlgren	31
White Oak	32
Naval Weapons Center	33
Naval Ship Research and Development Center	34
Naval Weapons Laboratory	35
Picatinny Arsenal	36
Redstone Arsenal	37
T.T.C.P. U.S. National Leader Panel W-2	38 - 41
Wright-Patterson Air Force Base, Library	42
American Institute of Aeronautics and Astronautics, Library	43
Pacific Technical Information Services, Northrop Institute of Technology	44
Department of Aerospace Engineering, Notre Dame University	45

	Copy No.
Applied Mechanics Reviews	46
Arnold Engineering Development Center	47
A.R.O. Incorporated	48
The Boeing Company, Library	49
General Dynamics Corporation, Library	50
Grumman Aerospace Corporation, Library	51
Lockheed Aircraft Corporation, Library	52
McDonnell-Douglas Corporation, Library	53
Martin-Marietta Corporation, Library	54
Rockwell International, Library	55
Sandia Corporation, Library	56
Sanders Associates, Nashua, New Hampshire	57
 In Canada	
Defence Research Establishment, Valcartier	58
N.A.E., Ottawa	59
T.T.C.P., Canadian National Leader Panel W-2	60 - 63
University of Toronto, Institute of Aerospace Studies	64
 In Europe	
A.G.A.R.D., Brussels	65
 In India	
Aeronautical Development Establishment, Bangalore	66
National Aeronautical Laboratories, Bangalore	67
 In Australia	
Department of Defence, Canberra	68
Defence Library, Campbell Park	69
Air Force Scientific Adviser	70
Army Scientific Adviser	71
Navy Scientific Adviser	72
Chief Defence Scientist	73
Executive Controller, Australian Defence Scientific Service	74
Controller, Policy and Programme Planning Division	75
Superintendent, Defence Science Administration Division	76
Defence Information Services Branch (for microfilming)	77

Copy No.

## Defence Information Services Branch for:

United Kingdom, Ministry of Defence, Defence Research Information Centre (DRIC)	78
United States, Department of Defense, Defense Documentation Center	79 - 90
Canada, Department of National Defence, Defence Science Information Service	91
New Zealand, Department of Defence	92
Australian National Library	93
Laboratory Programme Branch	94
Central Studies Establishment	95
Library, Aeronautical Research Laboratories	96
Library, Materials Research Laboratories	97
Director, Joint Intelligence Organisation	98
B.D.R.S.S., Canberra	99
Canadian Defence Science Information Service, Canadian High Commission, Canberra	100
N.A.S.A. Senior Scientific Representative, Canberra	101
U.S. Defense Documentation Center, via U.S. Embassy, Canberra	102 - 113
Chief Superintendent, Aeronautical Research Laboratories	114
Superintendent, Aerodynamics Division	115
Superintendent, Mechanical Engineering Division	116
Department of Industry and Commerce	
Government Aircraft Factories	117
R.A.A.F. Academy, Point Cook	118
C.A.C.	119

## INTERNAL

Director	120
Chief Superintendent, Weapons Research and Development Wing	121
Chief Superintendent, Applied Physics Wing	122
Chief Superintendent, Engineering Wing	123
Superintendent, Aerospace Division	124
Superintendent, Weapon Systems Division	125
Superintendent, Communications and Electronic Engineering Division	126
Superintendent, Systems Analysis Division	127
Head, Ballistics Composite	128
Principal Officer, Flight Research Group	129
Principal Officer, Ballistic Studies Group	130 - 131

	Copy No.
Principal Officer, Field Experiments Group	132
Principal Officer, Dynamics Group	133 - 135
Principal Officer, Aerodynamics Research Group	136
Principal Officer, Systems Modelling Group	137
Principal Officer, Terminal Guidance Group	138 - 139
Principal Officer, Control and Instrumentation Systems Group	140
Authors	141 - 142
A.D. Library	143 - 144
W.R.E. Library	145 - 146
Spares	147 - 166